

Glycoprotein Ib-binding Protein from the Venom of *Deinagkistrodon acutus* – cDNA Sequence, Functional Characterization, and Three-Dimensional Modeling

Yuh-Ling Chen[1], Kuo-Wei Tsai[1], Tschining Chang[1], Tse-Ming Hong[2], Inn-Ho Tsai[1, 3]

From the [1]Institute of Biological Chemistry and [2]Institute of Biomedical Sciences, Academia Sinica, [3]Institute of Biochemical Sciences, National Taiwan University, Taipei, Taiwan, Republic of China

Key words

Glycoprotein Ib, snake, modeling, C-lectin

Summary

Agkicetin-C, a potent glycoprotein Ib antagonist from the venom of the Chinese pit viper, Deinagkistrodon acutus, has been purified and characterized (5). It is a disulfide-linked heterodimer containing subunits of 132 and of 123 amino acid residues. Herein, the complete amino acid sequences were resolved by cloning and nucleotide sequencing of the cDNAs. The sequences of its subunits are homologous to those of other snake venom proteins of the C-type (Ca^{2+}-dependent) lectin superfamily. A three-dimensional model of agkicetin-C was constructed based on the crystal structure of habu coagulation factor IX/X-binding protein. By careful alignment of all the related sequences available and comparing the 3D-model of agkicetin-C with structures of other homologous proteins of different functions, some variable residues of agkicetin-C were identified, which possibly are responsible for the specificity of this distinct subtype of the C-type lectin-like venom proteins.

Introduction

Platelet adhesion and aggregation play important roles in homeostasis and thrombosis. The glycoprotein (GP) Ib-IX-V complex on the membrane of platelets functions as the primary receptor for von Willebrand factor (vWF) bound to the subendothelial matrix. The formation of the vWF-GPIb-IX-V complex regulates both the initial adhesion of platelets to the subendothelium at high shear and the shear-induced platelet aggregation which leads to thrombus formation (1).

A number of GPIb-binding proteins (GPIb-bp) have been isolated from various viperid snake venoms and characterized in the past few years (2), including alboaggregin-B (AL-B) from *Trimeresurus albolabris* (3), echicetin from *Echis carinatus* (4), agkicetin from *Deinagkistrodon acutus* (5), jararaca GPIb-BP from *Bothrops jararaca* (6), tokaracetin from *Trimeresurus tokarensis* (7), CHH-B from *Crotalus horridus horridus* (8), mamushigin from *Agkistrodon halys blomhoffii* (9), and crotalin from *Crotalus atrox* (10). Snake venom proteins specifically bind to the GPIb molecule at or in close proximity to the vWF-binding site, resulting in inhibition of platelet agglutination, with the exception of AL-B and mamushigin which induce agglutination of fixed human platelets without any cofactor. These proteins are disulfide-linked heterodimers containing subunits homologous to the carbohydrate-recognition domain (CRD) of the C-type lectins. They are classified into group VII of the lectins (11) along with pancreatic-associated proteins (12) and pancreatic-stone proteins (13). The C-type lectin-like superfamily from snake venom is comprised of GPIb-bp and other structurally similar proteins with diversified biological activities. For example, the venom of *Bothrops jararaca* contains at least four lectin-like proteins of different functions: jararaca IX/X-bp (14), two-chain botrocetin (15), bothrojaracin (16), and jararaca GPIb-binding protein (6). Jararaca IX/X-bp binds to coagulation factors IX and X in the presence of calcium ions (14). Botrocetin induces vWF binding to glycoprotein Ib (GPIb) of platelets (15). Bothrojaracin is a thrombin inhibitor binding the exosite of α-thrombin (16). Jararaca GPIb-BP is an antagonist specific to platelet GPIb (6). To ferret out the putative binding sites of these venom proteins for their targets will be important for mechanistic studies and drug design based on these proteins.

We have previously isolated agkicetin-C, a heterodimeric GPIb antagonist, from the venom of *Deinagkistrodon acutus* (the Five-pace pit viper) of China (5). Herein, the cDNAs encoding both subunits of agkicetin-C were cloned and sequenced to resolve the complete protein sequence. Moreover, a three-dimensional model of agkicetin-C was constructed using the x-ray crystallographic structure of habu IX/X-bp as a template (17). Some significant residues responsible for glycoprotein Ib-binding are proposed and discussed.

Materials and Methods

Materials

Crude venom and fresh venom glands of *D. acutus* from China were provided by Dr. M. Y. Liau (Institute of Preventive Medicine, Taiwan). Trifluoroacetic acid (TFA), acetonitrile, dithiothreitol, and 4-vinylpyridine were from Merck (Germany). Sequencing grade Lys-C endoproteinase was from Boehringer Mannheim (Germany). N-succinimidyl[2,3-^{3}H]propionate was purchased from Amersham (UK). Anti-GPIX mAb (MAB 1202) and anti-GPIbIIIa mAb (MAB 1207) were from Chemicon (USA). Anti-GPIb mAb (AK-2) was kindly supplied by Dr. Michael Berndt (Baker Medical Research Institute, Australia) (18). Human vWF was purified by the method of Fujimura et al. (19).

Platelet Agglutination Assay

Formaldehyde-fixed human platelets were prepared by the method of Peng et al. (3). The inhibitory effects of purified venom proteins on the agglutination

Correspondence to: Prof. Inn-Ho Tsai, Institute of Biological Chemistry, Academia Sinica, P. O. Box 23-106, Taipei, Taiwan 106, Republic of China – Tel.: 886-2-2362-0261 ext. 2011; Fax: 886-2-2363-5038; E-mail: bc201@gate.sinica.edu.tw

of fixed platelets induced by ristocetin (1.0 μg/ml) and human vWF (10 μg/ml) were measured using an aggregometer (Payton, module 600B, Canada) as previously descried (4).

Binding of ^{3}H-agkicetin to Fixed Platelets

Purified agkicetin-C was labeled by N-succinimidyl[2,3-^{3}H]propionate (20). The binding of ^{3}H-GPIb-bp to platelets was measured as previously described (4). The labeled protein was mixed with either buffer or unlabeled ligands, such as agkicetin or monoclonal antibody AK-2 before the addition of 200 ml platelet suspension. The mixture was incubated at 37° C for 10 min and then centrifuged at 12,000 × g for 2 min. The radioactivity of platelet pellets was measured by a β-counter (LKB 1219 Rackbeta, Sweden).

Reductive Alkylation and Amino Acid Sequencing

Purified GPIb-bp (50 μM) was denatured for 2.5 h in the dark in 0.25 M Tris-HCl buffer (pH 8.5) containing 6 M guanidine hydrochloride, 1 mM EDTA, and dithiothreitol (35 mM), under N_2 gas at 50° C. The protein was alkylated by adding iodoacetamide (105 mM) and incubated at room temperature for 30 min (21). S-alkylated subunits were purified by RP-HPLC using a Vydac C_8 column (0.46 × 25 cm). The elution was performed using a gradient of 0-30% acetonitrile (containing 0.07% TFA) over 10 min, followed by a gradient of 30-50% acetonitrile over 40 min. The effluent was monitored at 230 nm.

The alkylated α and β subunits of agkicetin-C were hydrolyzed by Lys-C endoproteinase as described previously (22). Digested peptides were separated by RP-HPLC on a Vydac C_{18} column (0.46 × 25 cm) and eluted with a linear gradient of acetonitrile in 0.07% trifluoroacetic acid at a flow rate of 1.0 ml/min. The effluent was monitored at 214 nm. After HPLC, the purified oligopeptides were subjected to mass analysis and amino acid sequencing. An automated gas-phase sequencer (Model 477A, Applied Biosystems, USA) was used, and the phenylthiohydantoin derivatives of amino acids were determined by an on-line HPLC system (23).

Ion Spray Mass Spectrometry (ISMS) Analysis

ISMS analysis was performed with a PE-Sciex API 100 mass analyzer. About 50 pmole of the purified proteins or peptides was dissolved in 25 μl of 50% acetonitrile containing 0.1% acetic acid and injected into the analyzer for positive mode analysis.

Cloning and Sequencing of Agkicetin-C

Two grams of fresh venom gland of *Deinagkistrodon acutus* (China) frozen previously in liquid nitrogen was ground to powder and then quickly suspended in 6 M guanidinium isothiocyanate, 5 mM sodium citrate (pH 7.0), 0.1 M β-mercaptoethanol, and 0.5% sarkosyl. This was homogenized on ice, and the cell lysate was centrifuged to remove cell debris. RNA in the supernatant was recovered (24). The poly(A) RNA was isolated according to the oligo-(dT) affinity method (25). A kit of cDNA synthesis from poly (A) RNA was used according to the manufacturer's instructions (Stratagene, USA).

Polymerase chain reaction (PCR) was conducted to amplify internal cDNAs of agkicetin-C. Two sets of degenerate oligonucleotide primers were designed based on the N-terminal amino acid sequences and internal peptide sequences determined for the purified agkicetin-C subunits. For PCR amplification of the α-subunit cDNA, the sense primer AN (a 21-mer designed from the N-terminal sequence DCLPGWS) and the antisense primer AC2 (a 20-mer designed from the peptide sequence KDTGFRT) were used. For PCR amplification of the β-subunit cDNA, oligonucleotide BN (a 22-mer designed from the N-terminal sequence DCPPDWS) as sense primer and oligonucleotide BC (a 22-mer designed from the peptide sequence NQWLSRAC) as antisense primer were synthesized. PCR was carried out using SuperTaq DNA polymerase (HT Biotechnology, UK) under the following conditions: a first step of 2 min at 92° C was followed by 30 cycles of 1 min at 92° C, 1 min at 55° C , and 1 min at 72° C, after which there was a further incubation for 10 min at 72° C. PCR products were subcloned by the dideoxythymidine-tailed vector method into a pGEM T-vector (Promega, USA).

DNA sequencing was performed with an automatic fluorescence-base sequencing of PCR-amplified templates using the model 373A DNA Sequencing System with a Taq DyeDeoxy terminator cycle sequencing kit (PE Biosystems, USA). The 3'-end of cDNA was determined from total RNA by rapid amplification of cDNA ends (RACE) method with RACE kit (Life Tech., USA). Based on the internal cDNA sequences, specific primers for the α subunit (5'-TACCAGCCCTTCAAGCTCCTC-3') and β subunit (5'-GATTGTCCCCCTGATTGGTCC-3') were also designed. The 5'-end of cDNA was determined by PCR using a sense primer (5'-TGCCTGGAACTTG-CAGACG-3') designed from the 5'-untranslated cDNA sequence of habu IX/X-bp (26) and two antisense primers (5'-ACGCGGTTTCAGGTACTTG-3' and 5'-TGCCTGGAACTTGCAGACG-3') designed from the internal cDNA sequence of α- and β-subunits of agkicetin-C, respectively.

Computer Modeling

The tertiary structure of agkicetin was constructed by a homology modeling technique based on satisfaction of spatial constraints derived from a high-resolution crystal structure of habu IX/X-bp (17) with the protein data base (PDB) entry as 1ixx. The sequences of both proteins were first aligned using the program BESTFIT of GCG (WI, USA, Package vers. 9.1). These were further manually adjusted by identifying sequence-conserved regions and disulfide bond-linking residues. The alignment showed protein sequence identities of up to 59% and 60% for the α and β subunits of agkicetin to those of IX/X-bp, respectively, and a deletion at position 59 in the α subunit of agkicetin. The alignment was introduced into the program Modeller (27) then integrated in InsightII (Molecular Simulations, USA) to construct a 3D model of agkicetin-C. Maximally satisfied coordinates were obtained without further manual intervention or subjective constraints. After the prototype model was built, the side chain conformations were refined by the program, SCWRL (28), with successive iterations of molecular dynamics followed by energy minimization using InsightII/ DISCOVER and AMBER force fields. The numbers of constraints applied to the protein were progressively reduced during subsequent cycles (29). Reliability of the model was assessed on a residue-by-residue basis using the programs, PROCHECK and WHAT IF (30, 31). Then program VERIFY 3D was used for further evaluation of 1D-to-3D compatibility (32). The results were fed back to the refinement parameters. Molecular dynamics, energy minimization, and side chain rotamer alternation were focused on defective regions of the model, followed by global optimization cycle by cycle until an optimized structure was obtained. The surface electrostatic properties of agkicetin-C were probed by the DelPhi program and then mapped onto the molecular surfaces of proteins viewed as contour maps (33).

Results

Inhibition of Platelet Agglutination by Agkicetin-C

The dose-dependent inhibitory effect of native agkicetin-C on ristocetin-vWF inducing platelet agglutination was shown in our previous report (5). The concentration of agkicetin-C required for 50% inhibition of agglutination of human platelets (IC_{50}) was approximately 12.5 nM. In contrast, agkicetin-C at 50 μg/ml showed no effect if the aggregation was induced by ADP (10 μM), collagen (5 μg/ml), or α-thrombin (0.1 U/ml). After reduction and alkylation, the subunits of the agkicetins were separated immediately by RP-HPLC on a Vydac C_8 column. The intact subunits were almost insoluble in Tris-saline buffer (TBS) alone, but soluble in TBS containing 4 M urea. The dissociated subunits (up to 10 μM) had no inhibitory activity on vWF-ristocetin-induced platelet agglutination (data not shown).

Binding of ^{3}H-agkicetin to Platelets

Agkicetin-C was labeled with N-succinimidyl[2,3-^{3}H]propionate without loss of antiplatelet activity. The binding of the labeled proteins to fixed human platelets was saturable, and was effectively inhibited by an excess (50 fold) of unlabeled agkicetins (Fig. 1A). The results of Scatchard analysis revealed that the binding sites of agkicetin-C were 24,900 ± 1900 per platelet, and the dissociation constant K_d was 16.8 ± 0.23 nM. Monoclonal antibody AK-2 could compete with the binding of labeled agkicetin-C to fixed platelets in a dose-dependent manner, and its IC_{50} was 2.8 μg/ml (Fig. 1B). Since the antibody is known to be specific for the N-terminal domain of GPIb (18), this domain seems to be involved in venom protein binding. In contrast, the monoclonal antibodies, MAB 1202 and MAB 1207 (against epitopes on the GPIX and the GPIIbIIIa, respectively), had no effect on the binding of agkicetin-C to platelets.

Various sugars at concentrations up to 100 mM did not affect the binding of agkicetin-C (15 nM) to fixed human platelets (Table 1). Polycations, such as poly-l-lysine, effectively inhibited agkicetin binding with an apparent IC_{50} of 7.5 μM, but polyanions, such as heparin, at up to 100 μM had no effect on agkicetin binding. Binding was also unaffected by EDTA, suggesting that binding is probably divalent-cation independent. However, increasing the ionic strength of the buffers by addition of sodium sulfate inhibited agkicetin binding. The IC_{50} for sodium sulfate was approximately 0.085 M (Table 1).

Table 1 Effect of various reagents on ^{3}H-agkicetin-C binding to human platelets

Reagent[a]	concentration	Binding of ^{3}H-agkicetin-C (% of control)[b]
D-Glucose	100 mM	103
D-Galactose	100 mM	100
D-Mannose	100 mM	104
D-Maltose	100 mM	103
D-Lactose	100 mM	102
N-Acetyl-D-glucosamine	100 mM	102
N-Acetylneuraminic acid	100 mM	104
Heparin	25 μM	99
(MW: 8000)	62 μM	93
	125 μM	85
Poly-L-lysine	1 μM	100
(MW: 10,000)	2 μM	83
	4 μM	74
	8 μM	47
	15 μM	8
EDTA	5 mM	99
Sodium sulfate	0.02 M	92
	0.05 M	87
	0.07 M	57
	0.10 M	24
	0.12 M	6

[a] Each reagent was mixed with ^{3}H-agkicetin-C and fixed human platelets (2×10^8 platelets/ml). The mixture was incubated at 37℃ for 5 min. Samples were centrifuged and radioactivities bound to the platelets were determinated. The concentrations indicated are the final concentrations.

[b] 100% binding indicates the specific binding of ^{3}H-agkicetin-C in Tris-saline buffer, pH 7.4.

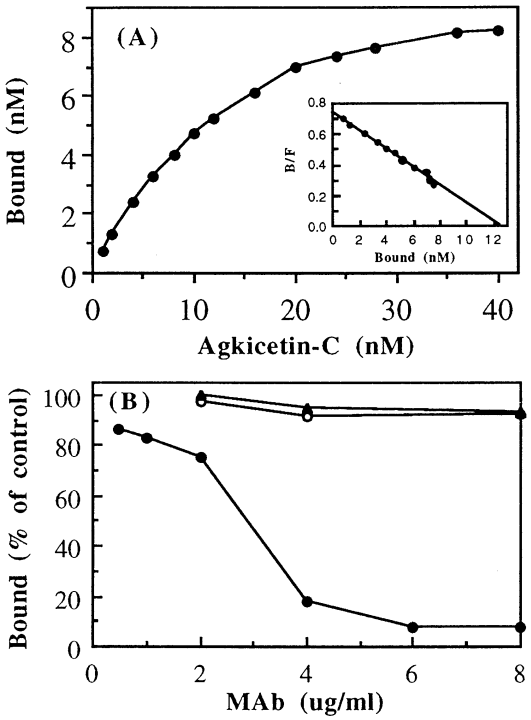

Fig. 1 Binding of agkicetin-C to fixed platelets. (A) Concentration-dependent binding of ^{3}H-agkicetin-C. The assay mixture contained 6.0×10^7 fixed platelets and ^{3}H-agkicetin in 200 μl buffer. After incubation for 10 min, it was centrifuged, and radioactivities of the pellets were counted. Total binding was measured in the absence of unlabeled proteins, while nonspecific binding was in the presence of 50-fold unlabeled protein. Specific binding of agkicetin-C (–●–) was calculated by subtracting nonspecific binding from total binding. (Inset) Scatchard plot of binding. (B) Effect of monoclonal antibodies. Platelet suspensions were incubated with ^{3}H-agkicetin-C (3.3 nM) and a monoclonal antibody: AK2 (–●–), MAB1202 (–▲–), or MAB1207 (–○–)

cDNA Cloning and Nucleotide Sequencing

Based on the amino acid sequences of the N-terminal region and those of the peptides, AK-9 or BK-8 derived from Lys-C hydrolysis, two pairs of sense and antisense primers were designed, and PCR was performed using Chinese *D. acutus* venom gland cDNA. The amplified PCR products were sequenced. cDNA fragments containing nucleotides 169-704 for the α subunit and nucleotides 130-685 for the β subunit were obtained by the 3'-RACE procedure. The 5' ends of the cDNAs were also amplified by PCR, and nucleotides 1-525 for the α subunit and nucleotides 1-498 for the β subunit were obtained. The full-length nucleotide sequences of agkicetin-C cDNA were assembled from the data of more than 3 clones from 3'-RACE and specific PCR. Fig. 2 shows the complete nucleotide sequences and the deduced amino acid sequences of agkicetin-C subunits. The 704-bp cDNA for the α subunit of agkicetin-C contains a 5'-untranslated region of 60 bp, an open reading frame of 465 bp, and a 3'-end noncoding region of 176 bp that includes a polyadenylation signal (AATAAA) and a poly (A) tail. The cDNA for the β subunit of 685 bp contains a 5'-untranslated region of 60 bp, an open reading frame of 438 bp, and a 3'-end noncoding region of 184 bp that includes a polyadenylation signal (AATAAA) and a poly (A) tail. The deduced amino acid sequences of the α and β-subunits contained a leader peptide of 23 amino acid residues, followed by a mature subunit of 132 and 123 residues, respectively. The underlined amino acid sequences are consistent with those

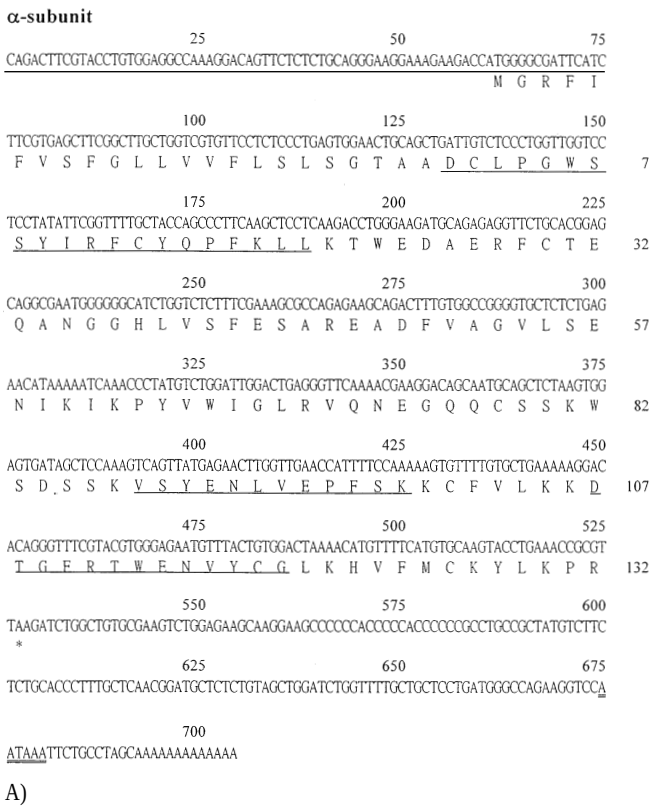

A)

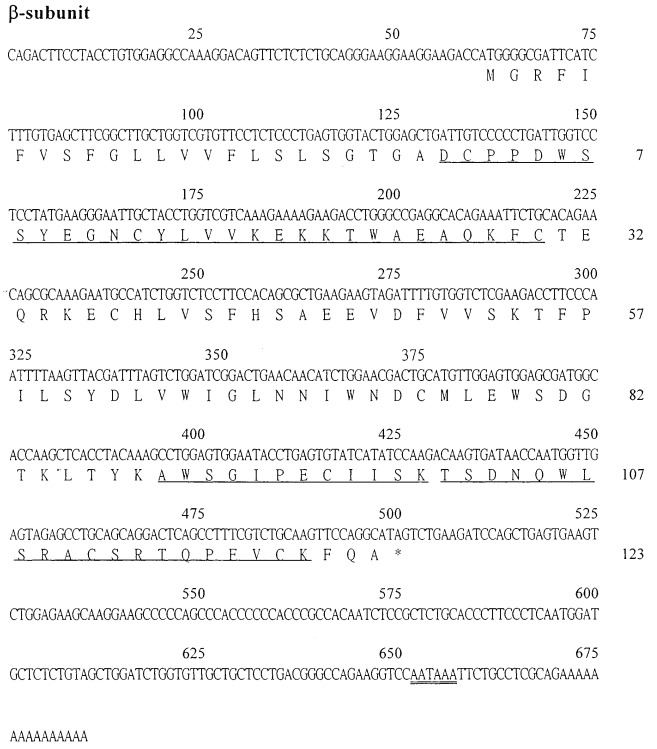

B)

Fig. 2 Nucleotide and amino acid sequences of the cDNAs encoding α- and β-subunits of agkicetin-C. Nucleotide numberings are above the nucleotide sequence, and amino acid numberings are given at the right side. The deduced amino acid sequences are shown in one-letter codes, and residues determined by protein sequencer are underlined. Asterisks and double-underlining denote termination codons and poly(A) addition signals, respectively. The sequence data are deposited in the GenBank database with the following accession numbers: AF102901 and AF102902

of HPLC-purified peptide fragments. The molecular mass of deduced S-carboxyamidated (SCA)-α- and β-subunits of agkicetin-C were calculated to be 15,781 and 14,743 Da, respectively. These values were confirmed by ISMS analysis of the purified SCA-subunits.

To test the possibility that the messengers of both chains of agkicetin-C are linked in tandem in the same RNA transcript, PCR amplification was performed on total RNAs isolated from the venom gland with a pair of specific primers (5' sense of one subunit and 3' antisense of another subunit). No PCR products encoding a double-sized precursor protein could be identified. The results suggest that the α and β subunits are coded by separate genes.

Homologous Modeling

A three-dimensional model of agkicetin-C was generated as mentioned in "Materials and Methods", and compared with the crystallographic structure of habu IX/X-bp (Fig. 3). A Ramachandran plot of main torsion angles generated by the program PROCHECK showed that 92% of the residues fall in the most favored regions. Only five residues fall outside the permissible regions. The energy profile over the entire sequence of the model is in the reasonably folded region, indicating that the agkicetin model is nativelike.

Discussion

Deinagkistrodon acutus (formerly *Agkistrodon acutus*) is a monotypic pit viper snake of medical importance due to its large size, frequent snakebites on humans, and wide range in South and East China. The venom causes strong hemorrhagic, antiplatelet, and anticoagulating effects due to various enzymes and non-enzymatic components. We have purified and characterized agkicetin-C from the venom of Chinese *D. acutus* (5). The antiplatelet effect of agkicetin appears to mediate specifically through its binding to the N-terminal domain of GPIb since it was replaced by a specific monoclonal antibody against GPIb (i.e., AK-2). As shown in Table 1, various sugars did not affect the binding of agkicetin-C to fixed human platelet; a lectin-like mechanism for agkicetin thus could be ruled out. Binding was also unaffected by EDTA, suggesting that binding probably is divalent-cation independent. However, increasing the ionic strength of the buffers by addition of sodium sulfate inhibited agkicetin binding. This is in accord with observations that platelet agglutination induced by alboaggregin-B and bovine vWF was dependent on ionic strength (3, 34). Positively charged polypeptides could interfere with the binding of ristocetin-mediated vWF to GPIb (35). We also found that polycations such as poly-L-lysine, but not polyanions (i.e., heparin), effectively inhibited agkicetin binding (Table 1).

Amino acid sequences of snake venom proteins of the C-lectin superfamily known to date show 44-70% identity (Fig. 4). The a subunit of agkicetin-C has the highest structural similarity (70%) to that of AL-B, and the β subunit bears the highest similarity (69%) to mamushigin β subunit. Interestingly, sequences of the leader peptides (Met^{-23}-Ala^{-1}) of all C-lectin-like venom proteins are almost identical. Sequences in the non-coding regions of venom proteins of the C-type lectin family generally bear higher similarities than those in their coding regions. Lower similarities in coding sequences relative to non-coding sequences of venom proteins may result from gene duplication and accelerated evolution of protein-coding regions to generate new functional subtypes. Positive Darwinian evolution has been well documented for other venom protein families including phospholipases

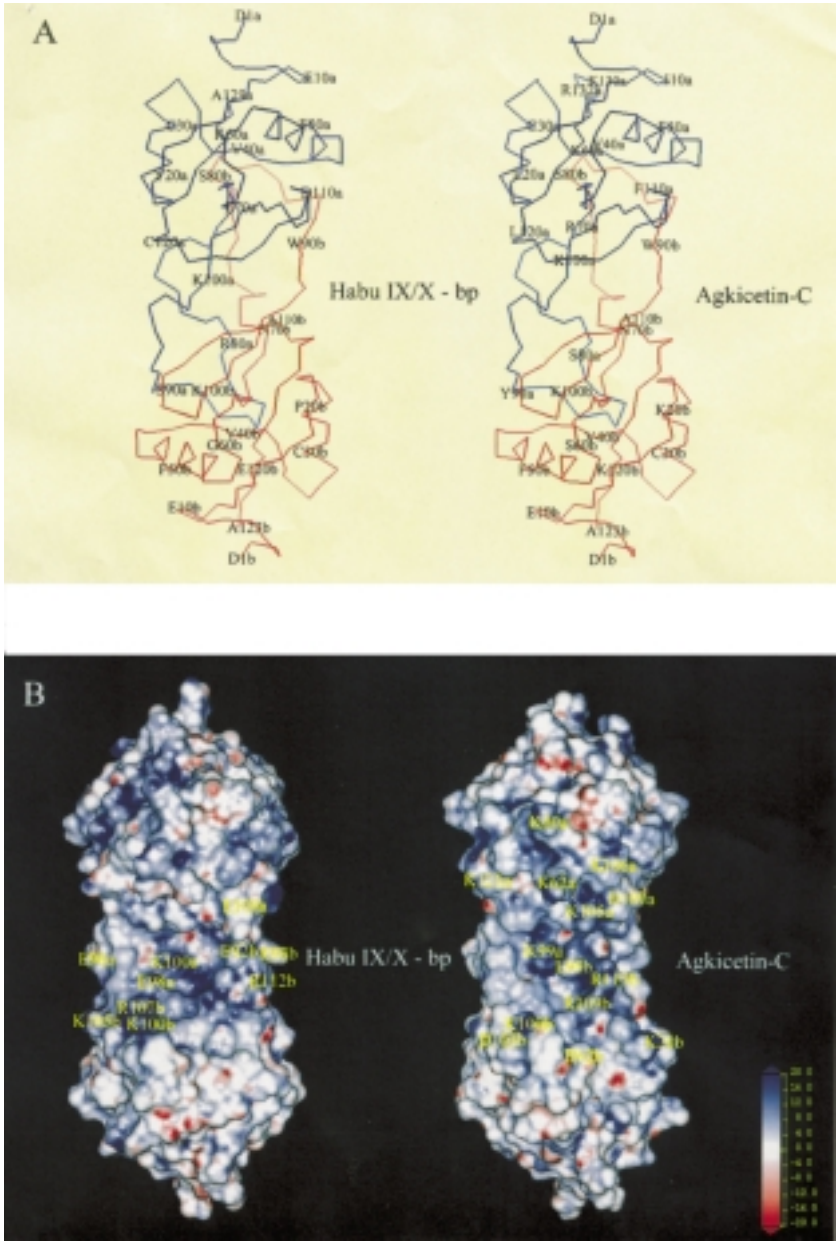

Fig. 3 Comparison of the 3D model of agkicetin-C to the structure of habu IX/X-bp. (A) α-Carbon backbones of the subunits α and β are shown in blue and red, respectively. Every 10th residue is marked. (B) Surface electrostatic potential maps. Orientation of the molecules is the same as that in (A). The putative binding sites in habu IX/X-bp (17, 38) and charged residues on agkicetin possibly participating in GPIb binding are marked. Residues belonging to subunits α or β are denoted respectively by letters a or b after the residue numbers. The color of electrostatic potential maps ranged from red (–20 k_BT/mol) via white (0 k_BT/mol) to blue (20 k_BT/mol), where k_B stands for Boltzmann's constant and T, absolute temperature

A_2, metalloproteases, serine proteases, and Elapidae non-enzymatic toxins (36, 37 and references therein).

The three-dimensional model of agkicetin-C which is based on the x-ray crystallographic structure of habu IX/X-bp is shown in Fig. 3A. In this model the backbone folds of both subunits of agkicetin-C are similar to each other, and their central regions project toward each other forming a tight association. The hydrophobic or core residues are highly conserved in the amino acid sequences of agkicetin and habu IX/X-bp, and they share 60% overall identity in protein sequences (Fig. 4). The only obvious main chain difference between the two is the C-terminal four residues extension in agkicetin, which is absent in habu IX/X-bp. The root mean square differences (RMSD values) for superposition of the Ca atoms between agkicetin and habu IX/X-bp are generally less than 0.3 Å.

Although the backbone structures of both venom proteins are very similar (Fig. 3A), the two molecules have quite different patterns of electrostatic surface potential, particularly at the concave surface created by the dimerization (Fig. 3B). The central region of the concave surface of habu IX/X-bp is much more basic (blue color) than that of agkicetin. The variable residues presumably are critical sites for their distinct functions. It was proposed previously that the putative binding sites of habu IX/X-bp for coagulation factors IX or X are located at this central concave surface, with Lys100 of subunit A and Lys100 and 105, Arg107, 109, and 112 of subunit B binding Gla-residues of the coagulation factors (17). In addition, some acidic residues of IX/X-bp, e.g., Glu96, 98, and 108 in subunit A and Glu92 and 93 in subunit B, are likely to coordinate Ca^{2+} ions (38). Noticeably, most of the corresponding positions in agkicetin are not charged (e.g., Phe97 of α subunit, and Gly92, Ile93, Gln105, Leu107, and Ser112 of β subunit). On the other hand, in the homologous mannose-binding protein, the five residues coordinating Ca^{2+} ion (i.e., Glu185, Asn187, Glu193, Asn205, and Asp206) (39, 40) are either deleted or changed in the corresponding positions in agkicetin-C. These sequence differences may explain why agkicetins do not require Ca^{2+} for activity,

α subunit

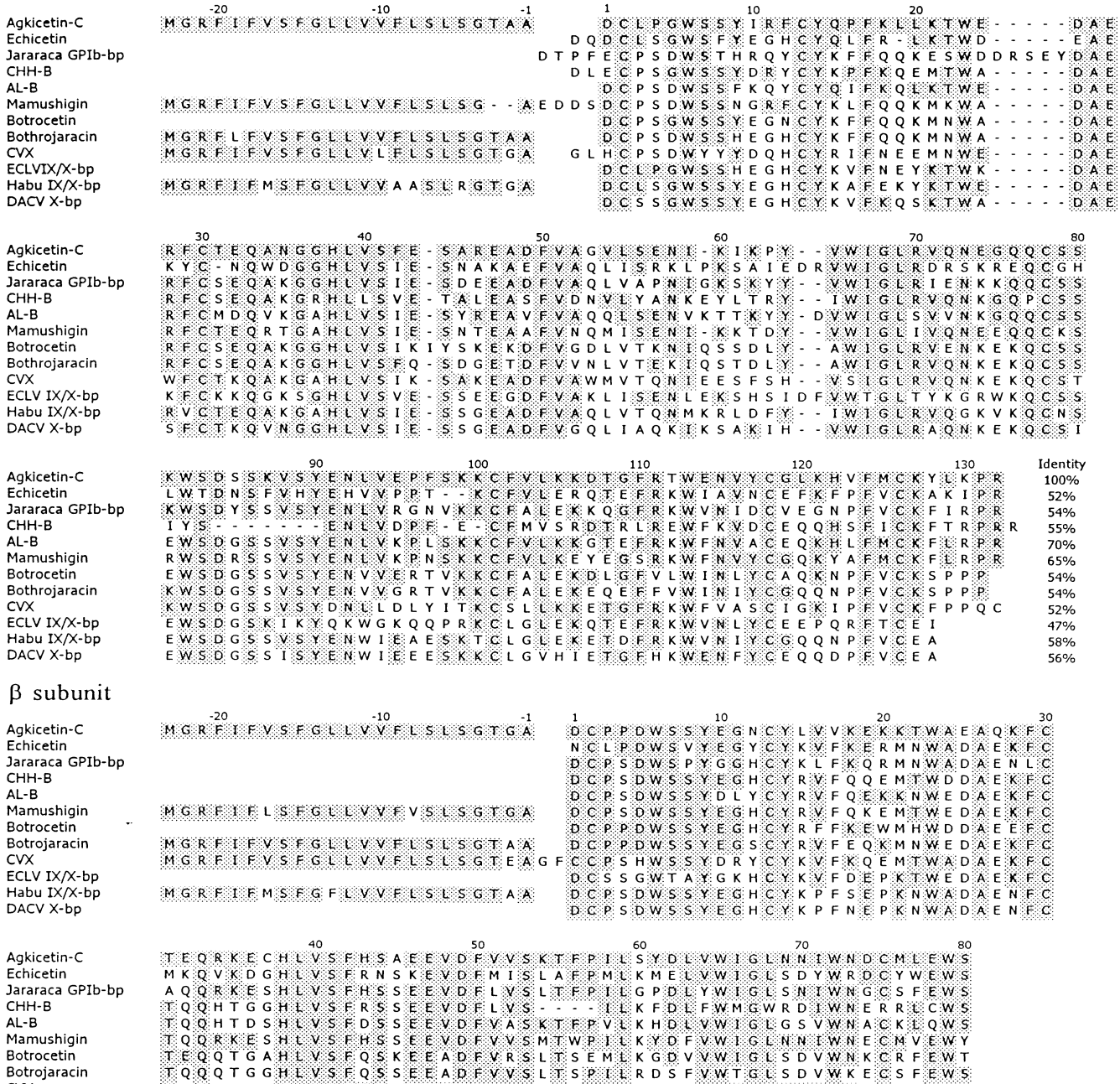

β subunit

Fig. 4 Sequence comparison of agkicetin-C-related venom proteins. Agkicetin-C to DACV X-bp are aligned by distinct functions: the first six specifically bind to GPIb; the latter three bind to vWF, thrombin, and p62/GPVI collagen receptor, respectively; and the last three bind to the coagulation factors IX or X. Amino acid numbering follows that of agkicetin-C. Gaps (–) are introduced to improve alignment. Identical residues are shaded. References are: echicetin from *Echis carinatus* venom (41, 42); jararaca GPIb-BP from *Bothrops jararaca* venom (43); CHH-B from *Crotalus horridus horridus* venom (8); alboaggregin-B (AL-B) from *Trimeresurus albolabris* venom (44); mamushigin from *Agkistrodon halys blomhoffii* venom (9); botrocetin from *Bothrops jararaca* venom (45); bothrojaracin from *Bothrops jararaca* venom (46); convulxin (CVX) from *Crotalus durissus terrificus* venom (47); ECLV IX/X-bp from *Echis carinatus leucogaster* venom (22); habu IX/X-bp from *Trimeresurus flavoviridis* venom (48); and DACV X-bp from *Deinagkistrodon acutus* venom (38)

and do not bind to carbohydrates nor to coagulation factors IX and X.

The salts with divalent anions (e.g., SO_4^{2+}) and polycations (e.g., polyLys) inhibited GPIb-binding (Table 1), electrostatic interactions are probably involved. Charged residues located on the subunit interface or the concave surface possibly involve in GPIb binding since separated subunits were inactive toward platelets. For example, surface basic residues at position 60, 62, 99, 105, and 106 of the a subunit and 21, 109, and 113 of the β subunit seem to constitute a continuous positively charged patch on the right side of the central concave surface of agkicetin-C in this 3D-model (Fig. 3B). Moreover, sequence alignment reveals that some surface residues such as Lys121 of the α subunit and Asp62, Glu95, and Asp103 of the β subunit are distinctly conserved in all GPIb-binding proteins (Fig. 4). However, these putative hypothesis and discussions based upon the results of modeling are highly speculative and remain to be investigated by crystallographic analyses and site-directed mutagenesis.

In conclusion, we have characterized and sequenced the glycoprotein Ib-binding protein (agkicetin-C) from *Deinagkistrodon acutus* venom. The proteins specifically block the vWF-GPIb interaction and are potential leads for designing novel anti-thrombotic drugs. The complete sequence and the three-dimensional model of agkicetin helps to explain its lack of binding capacity to coagulation factors and initiate some speculations on possible GPIb binding sites of the molecule. Hopefully, our results may serve as a basis for rational site-directed mutagenesis experiments of the venom GPIb-bps to explore their binding mechanism and structure-function relationships, which may contribute to the design of low molecular weight GPIb antagonists.

Acknowledgements

We thank Dr. Ming-Yi Liau (Taipei) for providing venom and venom glands, Dr. Michael Berndt (Australia) for the gift of monoclonal antibody AK-2, and our colleague Dr. Kay Hooi Khoo for critical reading of the manuscript.

References

1. Ware J. Molecular analyses of the platelet glycoprotein Ib-IX-V receptor. Thromb Haemost 1998; 79: 466-78.
2. Fujimura Y, Kawasaki T, Titani K. Snake venom proteins modulating the interaction between von Willebrand factor and platelet glycoprotein Ib. Thromb Haemost 1996; 76: 633-9.
3. Peng M, Lu W, Kirby EP. Alboaggregin-B: a new platelet agonist that binds to platelet membrane glycoprotein Ib. Biochemistry 1991; 30: 11529-36.
4. Peng M, Lu W, Beviglia L, Niewiarowski S, Kirby EP. Echicetin: a snake venom protein that inhibits binding of von Willebrand factor and alboaggregins to platelet glycoprotein Ib. Blood 1993; 81: 2321-8.
5. Chen YL, Tsai IH. Functional and sequence characterization of agkicetin, a new glycoprotein Ib antagonist isolated from *Agkistrodon acutus* venom. Biochem Biophys Res Commun 1995; 210: 472-7.
6. Fujimura Y, Ikeda Y, Miura S, Yoshida E, Shima H, Nishida S, Suzuki M, Titani K, Taniuchi Y, Kawasaki T. Isolation and characterization of jararaca GPIb-BP, a snake venom antagonist specific to platelet glycoprotein Ib. Thromb Haemost 1995; 74: 743-50.
7. Kawasaki T, Taniuchi Y, Hisamichi N, Fujimura Y, Suzuki M, Titani K, Sakai Y, Kaku S, Satoh N, Takenaka T, Handa M, Sawai Y. Tokaracetin, a new platelet antagonist that binds to platelet glycoprotein ib and inhibits von Willebrand factor-dependent shear-induced platelet aggregation. Biochem J 1995; 308: 947-53.
8. Andrews RK, Kroll MH, Ward CM, Rose JW, Scarborough RM, Smith AI, Lopez JA, Berndt MC. Binding of a novel 50-kilodalton alboaggregin from *Trimeresurus albolabris* and related viper venom proteins to the platelet membrane glycoprotein Ib-IX-V complex. Effect on platelet aggregation and glycoprotein Ib-mediated platelet activation. Biochemistry 1996; 35: 12629-39.
9. Sakurai Y, Fujimura Y, Kokubo T, Imamura K, Kawasaki T, Handa M, Suzuki M, Matsui T, Titani K, Yoshioka A. The cDNA cloning and molecular characterization of a snake venom platelet glycoprotein Ib-binding protein, mamushigin, from *Agkistrodon halys* blomhoffii venom. Thromb Haemost 1998; 79: 1199-207.
10. Chang MC, Lin HK, Peng HC, Huang TF. Antithrombotic effect of crotalin, a platelet membrane glycoprotein Ib antagonist from venom of *Crotalus atrox*. Blood 1998; 91: 1582-9.
11. Drickamer K. Evolution of Ca(2+)-dependent animal lectins. Prog Nucleic Acid Res Mol Biol 1993; 45: 207-32.
12. Orelle B, Keim V, Masciotra L, Dagorn JC, Iovanna JL. Human pancreatitis-associated protein. Messenger RNA cloning and expression in pancreatic diseases. J Clin Invest 1992; 90: 2284-91.
13. Giorgi D, Bernard JP, Rouquier S, Iovanna J, Sarles H, Dagorn JC. Secretory pancreatic stone protein messenger RNA. Nucleotide sequence and expression in chronic calcifying pancreatitis. J Clin Invest 1989; 84: 100-6.
14. Sekiya, F, Atoda, H, Morita T. Isolation and characterization of an anticoagulant protein homologous to botrocetin from the venom of *Bothrops jararaca*. Biochemistry 1993; 32: 6892-7.
15. Fujimura Y, Titani K, Usami Y, Suzuki M, Oyama R, Matsui T, Fukui H, Sugimoto M, Ruggeri ZM. Isolation and chemical characterization of two structurally and functionally distinct forms of botrocetin, the platelet coagulatinin isolated from the venom of *Bothrops jararaca*. Biochemistry 1991; 30: 1957-64.
16. Zingali RB, Jandrot-Perrus M, Guillin MC, Bon C. Bothrojaracin, a new thrombin inhibitor isolated from *Bothrops jararaca* venom: characterization and mechanism of thrombin inhibition. Biochemistry 1993; 32: 10794-802.
17. Mizuno H, Fujimoto Z, Koizum M, Kano H, Atoda H, Morita T. Structure of coagulation factors IX/X-binding protein, a heterodimer of C-type lectin domains. Nature Struc Biol 1997; 4: 438-41.
18. Chong BH, Fawaz I, Chesterman CC, Berndt MC. Heparin-induced thrombocytopenia: mechanism of interaction of the heparin-dependent antibody with platelets. Br J Haemat 1989; 73: 235-40.
19. Fujimura Y, Titani K, Lolland LZ, Russell SR, Roberts JR, Elder JH, Ruggeri ZM, Zimmerman TS. Von Willebrand factor. A reduced and alkylated 52/48-kDa fragment beginning at amino acid residue 449 contains the domain interacting with platelet glycoprotein Ib. J Biol Chem 1986; 261: 381-5.
20. Bolton AE, Hunter WM. The labeling of proteins to high specific radioactivities by conjugation to a ^{125}I-containing acylating agent. Biochem J 1973; 133: 529-39.
21. Ozols J. Amino acid analysis. Methods Enzymol 1990; 182: 587-601.
22. Chen YL, Tsai IH. Functional and sequence characterization of coagulation factor IX/factor X-binding protein from the venom of *Echis carinatus leucogaster*. Biochemistry 1996; 35: 5264-71.
23. Hunkapiller MW, Hewick RM, Dreyer WJ, Hood LE. High-sensitivity sequencing with a gas-phase sequenator. Methods Enzymol 1983; 91: 399-412.
24. Chirgwin JM, Przybyla AE, MacDonald RJ, Rutter WJ. Isolation of biologically active ribonucleic acid from sources enriched in ribonuclease. Biochemistry 1979; 18: 5294-9.
25. Aviv H, Leder P. Purification of biologically active globin messenger RNA by chromatography on oligothymidylic acid-cellulose. Proc Natl Acad Sci USA 1972; 69: 1408-12.
26. Matsuzaki R, Yoshiara E, Yamada M, Shima K, Atoda H, Morita T. cDNA cloning of IX/X-BP, a heterogeneous two-chain anticoagulant protein from snake venom. Biochem Biophys Res Commun 1996; 220: 382-7.

27. Šali A, Blundell TL. Comparative protein modeling by satisfaction of spatial restraints. J Mol Biol 1993; 234: 779-815.
28. Bower MJ, Cohen FE, Dunbrack RL Jr. Prediction of protein side-chain rotamers from a backbone-dependent rotamer library: a new homology modeling tool. J Mol Biol 1997; 267: 1268-82.
29. Vinals C, De Bolle X, Depiereux E, Feytmans E. Knowledge-based modeling of the D-lactate dehydrogenase three-dimensional structure. Proteins 1995; 21: 307-18.
30. Laskowski RA, Moss DS, Thornton JM. Main-chain bond lengths and bond angles in protein structures. J Mol Biol 1993; 231:1049-67.
31. Vriend G. WHAT IF: a molecular modeling and drug design program. J Mol Graph 1990; 8: 52-6.
32. Luthy R, Bowie JU, Eisenberg D. Assessment of protein models with three-dimensional profiles. Nature 1992; 356: 83-5.
33. Honig B, Nicholls A. Classical electrostatics in biology and chemistry. Science 1995; 268: 1144-9.
34. Cooper HA, Wilkins KW Jr, Johnson PR Jr, Wagner RH. Platelet-aggregating factor and the aggregation of fixed washed platelets. J Lab Clin Med 1977; 90: 512-21.
35. Hoylaerts MF, Nuyts K, Peerlinck K, Deckmyn H, Vermylen J. Promotion of binding of von Willebrand factor to platelet glycoprotein Ib by dimers of ristocetin. Biochem J 1995; 306: 454-63.
36. Chang LS, Lin J, Chou YC, Hong E. Genomic structures of cardiotoxin 4 and cobrotoxin from *Naja naja atra* (Taiwan cobra). Biochem Biophys Res Commun 1997; 239: 756-62.
37. Deshimaru M, Ogawa T, Nakashima K, Nobuhisa I, Chijiwa T, Shimohigashi Y, Fukumaki Y, Niwa M, Yamashina I, Hattori S, Ohno M. Accelerated evolution of Crotalinae snake venom gland serine proteases. FEBS Lett 1996; 397: 83-8.
38. Atoda H, Ishikawa M, Mizuno H, Morita T. Coagulation factor X-binding protein from *Deinagkistrodon acutus* venom is a Gla domain-binding protein. Biochemistry 1998; 37: 17361-70.
39. Weis WI, Kahn R, Fourme R, Drickamer K, Hendrickson WA. Structure of the calcium-dependent lectin domain from a rat mannose-binding protein determined by MAD phasing. Science 1991; 254: 1608-15.
40. Weis WI, Drickamer K, Hendrickson WA. Structure of a C-type mannose-binding protein complexed with an oligosaccharide. Nature 1992; 360: 127-34.
41. Peng M, Holt JC, Niewiarowski S. Isolation, characterization and amino acid sequence of echicetin beta subunit, a specific inhibitor of von Willebrand factor and thrombin interaction with glycoprotein Ib. Biochem Biophys Res Commun 1994; 205: 68-72.
42. Polgar J, Magnenat EM, Peitsch MC, Wells TNC, Saqi MSA, Clemetson KJ. Amino acid sequence of the alpha subunit and computer modeling of the alpha and beta subunits of echicetin from the venom of *Echis carinatus* (saw-scaled viper). Biochem J 1997; 323: 533-7.
43. Kawasaki T, Fujimura Y, Usami Y, Suzuki M, Miura S, Sakurai Y, Makita K, Taniuchi Y, Hirano K, Titani K. Complete amino acid sequence and identification of the platelet glycoprotein Ib-binding site of jararaca GPIb-BP, a snake venom protein isolated from *Bothrops jararaca.* J Biol Chem 1996; 271: 10635-9.
44. Usami Y, Suzuki M, Yoshida E, Sakurai Y, Hirano K, Kawasaki T, Fujimura Y, Titani K. Primary structure of alboaggregin-B purified from the venom of *Trimeresurus albolabris.* Biochem Biophys Res Commun 1996; 219: 727-33.
45. Usami Y, Fujimura Y, Suzuki M, Ozeki Y, Nishio K, Fukui H, Titani K. Primary structure of two-chain botrocetin, a von Willebrand factor modulator purified from the venom of *Bothrops jararaca.* Proc Natl Acad Sci USA 1993; 90: 928-32.
46. Arocas V, Castro HC, Zingali RB, Guillin MC, Jandrot-Perrus M, Bon C, Wisner A. Molecular cloning and expression of bothrojaracin, a potent thrombin inhibitor from snake venom. Eur J Biochem 1997; 248: 550-7.
47. Leduc M, Bon C. Cloning of subunits of convulxin, a collagen-like platelet-aggregating protein from *Crotalus durissus terrificus* venom. Biochem J 1998; 333: 389-93.
48. Atoda H, Hyuga M, Morita T. The primary structure of coagulation factor IX/factor X-binding protein isolated from the venom of *Trimeresurus flavoviridis.* Homology with asialoglycoprotein receptors, proteoglycan core protein, tetranectin, and lymphocyte Fc epsilon receptor for immunoglobulin E. J Biol Chem 1991; 266: 14903-11.

Received July 12, 1999 Accepted after revision September 23, 1999